

Implications of Surfactant-Induced Flow for Miscible-Displacement Estimation of Air–Water Interfacial Areas in Unsaturated Porous Media

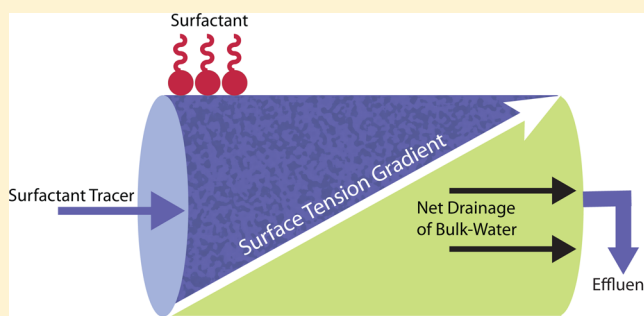
Molly S. Costanza-Robinson,^{*,†} Zheng Zheng,[†] Eric J. Henry,[‡] Benjamin D. Estabrook,[†] and Malcolm H. Littlefield[†]

[†]Program for Environmental Studies and Department of Chemistry and Biochemistry, Middlebury College, 287 Bicentennial Way, Middlebury, Vermont 05753, United States

[‡]Department of Geography and Geology, University of North Carolina—Wilmington, 601 South College Road, Wilmington, North Carolina 28403, United States

S Supporting Information

ABSTRACT: Surfactant miscible-displacement experiments represent a conventional means of estimating air–water interfacial area (A_i) in unsaturated porous media. However, changes in surface tension during the experiment can potentially induce unsaturated flow, thereby altering interfacial areas and violating several fundamental method assumptions, including that of steady-state flow. In this work, the magnitude of surfactant-induced flow was quantified by monitoring moisture content and perturbations to effluent flow rate during miscible-displacement experiments conducted using a range of surfactant concentrations. For systems initially at 83% moisture saturation (S_w), decreases of 18–43% S_w occurred following surfactant introduction, with the magnitude and rate of drainage inversely related to the surface tension of the surfactant solution. Drainage induced by 0.1 mM sodium dodecyl benzene sulfonate, commonly used for A_i estimation, resulted in effluent flow rate increases of up to 27% above steady-state conditions and is estimated to more than double the interfacial area over the course of the experiment. Depending on the surfactant concentration and the moisture content used to describe the system, A_i estimates varied more than 3-fold. The magnitude of surfactant-induced flow is considerably larger than previously recognized and casts doubt on the reliability of A_i estimation by surfactant miscible-displacement.



INTRODUCTION

Air–water interfacial area in unsaturated porous media is an important parameter that influences equilibrium solute and colloid retention, as well as the kinetics of interphase mass and energy transfer. For example, depending on system conditions, up to 90% of the observed retardation of various volatile organic compounds has been attributed to adsorption at the air–water interface.^{1–3} Numerous methods have been developed for experimental estimation of air–water interfacial area, including a variety of long-chain alcohol and surfactant-based aqueous tracer methods,^{1,4–8} gas-phase tracer methods,^{3,9–12} and most recently, high-resolution imaging techniques.^{13–16} The application of these methods has aided our understanding of the functional dependence of the air–water interface on porous media and system properties (e.g., moisture content, media surface area, wetting-drying hysteresis) but has also revealed that estimated interfacial areas for similar porous media systems vary, depending on the measurement method used.^{9,11,14–17} Limitations to various measurement methods have been proposed to account for the method-dependence, including that imaging methods may not capture interfacial area

associated with surface roughness due to image resolution constraints¹⁸ and that both gas- and aqueous-phase tracers may not fully access all regions of the air–water interface.^{7,11,12,19} However, potentially significant limitations of the surfactant miscible-displacement interfacial tracer method have not been previously investigated. Careful assessment of this method is particularly important, because air–water interfacial area estimations and interfacial trends obtained by its application^{1,8,17,20} have served as a baseline for comparison in numerous experimental and modeling investigations of the air–water interface.^{7,11,15,16,19,21–29}

The surfactant miscible-displacement method is a column-scale technique that involves displacing surfactant-free resident pore water with a surfactant-containing tracer solution and correlating the arrival time of the surfactant (interfacial tracer) to the air–water interfacial area. The introduction of the

Received: December 6, 2011

Revised: September 18, 2012

Accepted: September 20, 2012

Published: October 3, 2012

surfactant to the system creates a surface tension difference between adjacent surfactant-containing and surfactant-free regions, which can result in capillary pressure gradients, as described by the Young–Laplace equation.³⁰ Consequently, the introduction of a surfactant can induce flow of bulk water in the system. Henry and Smith³¹ have reviewed experimental work and numerical modeling related to surfactant-induced unsaturated flow, noting that flow tends to occur from higher surfactant concentration (lower surface tension, less negative soil–water pressure) regions toward lower concentration (higher surface tension, more negative soil–water pressure) regions. Therefore, in a surfactant miscible-displacement experiment, surfactant-induced flow would manifest as drainage of pore water from the inlet of the column toward the column outlet, an effect that would propagate through the column with the advancing surfactant solute front. Although surfactant-induced flow has been studied in detail,^{31,32} the influence of surfactant-induced flow on miscible-displacement interfacial area measurements has not previously been assessed.

Surfactant-induced flow would present multiple interrelated complications for miscible-displacement air–water interfacial area determination. First, because moisture content and (total) air–water interfacial area (i.e., capillary + film) are inversely related over moisture content ranges typical of natural systems, surfactant-induced drainage of water from the column would serve to increase the interfacial area during the measurement. Additionally, surfactant-induced flow would violate the method assumptions of constant moisture content and steady-state flow and, in doing so, could alter the transport of the surfactant through the porous media system. Because the arrival time of the surfactant forms the basis for interfacial area determination, any alteration to surfactant transport is likely to influence the estimated interfacial area. Despite recognition of the theoretical potential for surface tension effects to influence surfactant miscible-displacement air–water interfacial area measurement and recommendations in the literature to keep surface tension gradients to a minimum,^{7,20} neither the magnitude of surfactant-induced flow during conventional surfactant miscible-displacement experiments nor its implications for interfacial area estimation have been examined.

In this work, surfactant miscible-displacement experiments were conducted for a natural sandy medium using a range of surfactant concentrations in order to investigate the occurrence, magnitude, and nature of surfactant-induced flow under conditions typical of those used in air–water interfacial area estimation. The implications of surfactant-induced flow, including transience in system moisture content and enhanced solute transport, for surfactant miscible-displacement interfacial area determination are examined.

EXPERIMENTAL SECTION

Materials. The porous medium used for this study was a natural silica sand (Unimin Corporation, Emmett, ID), referred to in earlier work as Granusil Mix.^{15,33} Relevant properties of the sand and unsaturated packing are shown in Table 1. Pentafluorobenzoate (PFBA, 0.47 mM) as pentafluorobenzoic acid (Arcos Organics, 99% purity) and bromide (0.35 mM) as NaBr (Sigma Aldrich, 99% purity) were used as nonreactive tracers. The anionic surfactant dodecylbenzene sulfonate (SDBS, 0.05–0.20 mM) (Arcos Organics, 88% purity) as a sodium salt was used as the interfacial tracer. NaCl (Sigma Aldrich, 99% purity) was used as a background electrolyte in all tracer solutions, as well as in tracer-free solutions that were

Table 1. Select Properties of the Porous Medium and Column Packing

average particle size	211 μm
uniformity coefficient, U (d_{60}/d_{10})	2.95
volume-normalized N_2 /BET surface area ^a	5175 cm^{-1}
volume-normalized geometric surface area, SA^b	163 cm^{-1}
bulk density	1.64 g/cm^3
porosity	0.391

^aCalculated as surface area per unit bulk system volume (cm^2/cm^3).

^bCalculated under the assumption of smooth spheres, calculated as $SA = 6(1 - n)/d_{50}$ where n is porosity and d_{50} is the median particle diameter.

used to establish the desired initial column moisture conditions and to elute tracers from the system. NaCl concentrations in tracer-background and tracer-free solutions were selected to establish a 10.8 mM total Na^+ concentration. Tracer and electrolyte compounds and concentrations reflect those commonly used in A_1 determination.

Miscible-Displacement Experiments. Most miscible-displacement experiments were conducted in sequential-tracer mode, in which the nonreactive tracer was introduced and eluted separately and prior to an analogous SDBS pulse. A simultaneous-tracer experiment was also conducted, in which the nonreactive tracer and SDBS were introduced as a single mixed solution, following a baseline experiment using the nonreactive tracer only. Experiments were conducted for systems that were initially “wet” or “dry”, and select experiments were performed in duplicate to confirm reproducibility. A summary of experimental conditions is provided in Table 2.

The porous medium was dry-packed in a stainless steel column (10-cm \times 5-cm i.d.) (Grace Discovery Sciences), and a single packing was used for all experiments. The lower column end-cap contained stainless steel bed support and flow-distributor frits and a nylon capillary membrane (Soil Measurement Systems, air entry > 700 cm- H_2O). The upper column end-cap contained only the bed support and flow distributor frits, allowing transmission of both air and water. All system connections and seals were stainless steel or PTFE. To saturate the system, tracer-free solution was introduced to the column using an HPLC pump connected to the bottom of a vertically oriented column, and upward flow was continued until the column mass stabilized. The desired initial moisture content for the miscible-displacement experiment was established using an HPLC pump to deliver a constant downward flux of tracer-free solution to the top of the column and a hanging water column to establish a constant pressure head at the lower column boundary. Specific boundary conditions were selected to establish a relatively uniform initial moisture profile (described in Supporting Information). The same boundary conditions used to establish initial moisture conditions were maintained throughout a given miscible-displacement experiment. Tracer input continued until influent and effluent tracer concentrations were equal, or, in cases where tracer transport was not monitored, until no further drainage was detected. Tracers were eluted from the system using tracer-free solution. The system was resaturated and redrained to the desired initial moisture content to begin each experiment.

Data Collection. Changes in the column-average moisture content and effluent flow rates during experiments were monitored using a datalogging balance to record column

Table 2. Summary of Experiments

[SDBS], mM	γ (mN/m)	K_D (cm ³ /g)	$K_{IW} \times 10^{-3}$ (cm)	exp conditions ^a	R	θ_w^b			A_I (cm ⁻¹) ^c	
						initial	average	final	initial	average
0.05	52.9	0.202	5.82	wet/sequential	3.21	0.319	0.282	0.252	65	51
0.1	48.0	0.105	2.91	wet/sequential	2.59	0.299	0.229	0.195	104	65
0.1	48.0	0.105	2.91	wet/sequential	2.24	0.339	0.262	0.227	85	52
0.1	48.0	0.105	2.91	dry/sequential ^d	—	0.193	—	0.129	—	—
0.1	48.0	0.105	2.91	wet/simultaneous ^d	—	0.294	—	0.124	—	—
0.2	43.0	0.063	1.46	wet/sequential	1.73	0.314	0.202	0.161	86	30
0.2	43.0	0.063	1.46	wet/sequential	1.77	0.325	0.204	0.165	101	37

^aRefers to nominally wet vs dry initial moisture conditions and sequential vs simultaneous tracer introduction. ^bInitial, time-averaged, and final average volumetric water content determined using nonreactive tracer arrival time, using column mass loss, averaged over time prior to SDBS $C/C_0 = 1$, and using final column mass, respectively; ^cCalculated using eq 3, using initial or time-averaged θ_w . ^dSDBS transport was not monitored and thus R, average θ_w , and A_I were not calculated.

mass at 5-min intervals. Because the column was at a steady-state flow condition prior to the introduction of tracers, and because the applied flux at the inlet boundary remained constant during tracer application, any change in column mass, and thus moisture content and effluent flow rate, was caused by the introduction of the surfactant interfacial tracer (i.e., surfactant-induced flow). Density differences among tracer-free, nonreactive tracer, and surfactant tracer solutions were negligible (<2%), such that tracer concentrations in the column and effluent solution did not influence these measurements. PFBA and SDBS concentrations in the column effluent were determined at 5-min intervals via absorbance at 230 nm using inline UV/vis spectrophotometry (Agilent 8453 UV/vis). Bromide concentrations were determined for discrete effluent samples using a bromide ion selective electrode (Thermo Orion Ionplus combination electrode).

Data Analysis. Because they may not be the same, *actual* air–water interfacial areas in the system (i.e., the physical reality), referred to herein simply as “interfacial areas”, are distinguished from experimentally estimated air–water interfacial areas, which will be referred to by the symbol, A_I . Moreover, all interfacial areas discussed herein, whether estimated or actual, refer to total areas (i.e., capillary + film interfacial contributions). Arrival times (t_{tracer}) for nonreactive tracers and SDBS were determined as the area above tracer breakthrough curve arrival waves:

$$t_{\text{tracer}} = \sum_{t=0}^{t=p} \left(1 - \left(\frac{C^n + C^{n+1}}{2C_0} \right) \right) (t^{n+1} - t^n) \quad (1)$$

where C^n and C^{n+1} refer to effluent tracer concentrations at two consecutive time points, t^n and t^{n+1} ; C_0 is the tracer input concentration, and p is the tracer input pulse duration. The ratio of SDBS (t_{SDBS}) and nonreactive tracer ($t_{\text{nonreactive}}$) arrival times is the retardation factor (R):

$$R = \frac{t_{\text{SDBS}}}{t_{\text{nonreactive}}} \quad (2)$$

where SDBS retardation is due to accumulation at the solid mineral surfaces and at the air–water interface:

$$R = 1 + \frac{\rho_b K_D}{\theta_w} + \frac{A_I K_{IW}}{\theta_w} \quad (3)$$

where the “1” accounts for nonreactive tracer transport, ρ_b is the bulk density of the porous medium (g/cm³), K_D is the solid-phase sorption coefficient (cm³/g), θ_w is the effective

volumetric water content (—), A_I is the estimated volume-normalized total air–water interfacial area (area of total interface per system volume, cm⁻¹), and K_{IW} is the interfacial adsorption constant (cm). A_I was calculated from eq 3 using measured SDBS K_D and K_{IW} values, known ρ_b , and, as is convention for A_I determination, the column-average θ_w determined using the arrival time of the nonreactive tracer. Methods and results for K_D and K_{IW} determination are described in the Supporting Information.

RESULTS AND DISCUSSION

Surfactant-Induced Drainage. Figure 1 shows column-average moisture saturation (S_w) over time for a representative

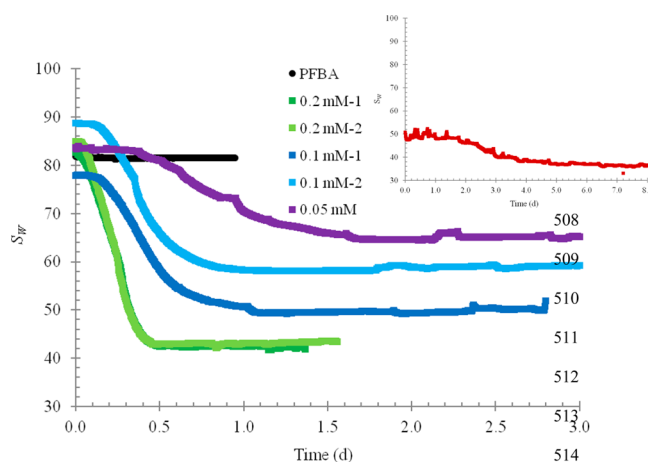


Figure 1. Column-average S_w versus time during sequential-tracer PFBA (representative) and SDBS (0.5–0.2 mM) experiments for wet systems. The 0.2 mM replicate experiments (light and dark green) overlap. Inset data are for 0.1 mM SDBS in a dry system (note the extended time axis).

PFBA experiment and all “wet” SDBS experiments. Introducing PFBA to the system had no effect on system moisture content, as expected, given that PFBA is not surface-active. In contrast, as the applied low surface tension SDBS solution displaced high surface tension surfactant-free resident pore water, S_w decreases of 18–43% were observed in the initially wet (~83% S_w) systems. The magnitude of surfactant-induced drainage was highly reproducible for a given surfactant input concentration and was inversely and linearly related to the surface tension of the influent SDBS solution (Figure 2). Also shown in the inset of Figure 1 is S_w behavior for a “dry” system with an initial S_w

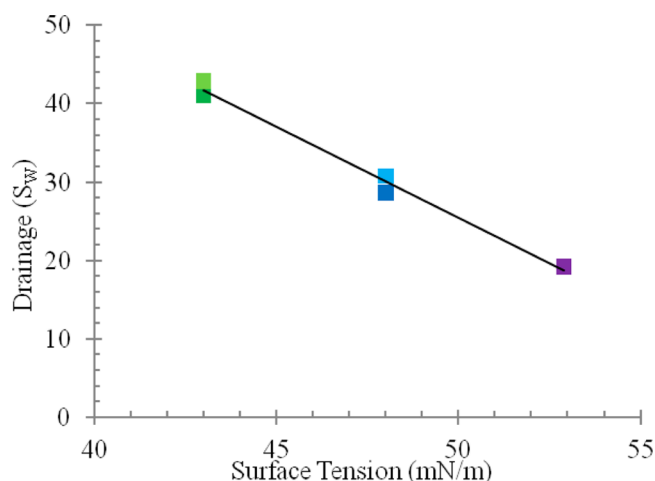


Figure 2. Observed drainage for wet systems, expressed as the decrease in S_w , as a function of the surface tension of the influent SDBS solution. Colors are used as in Figure 1.

of 51%, which confirms that surfactant-induced flow effects are not confined to systems with high initial moisture content. The S_w decrease induced by 0.1 mM SDBS in the dry system was roughly half of that observed for the corresponding wet system, but still significant. In fact, regardless of initial moisture content, the drainage induced by 0.1 mM SDBS, a concentration commonly used for miscible-displacement determination of A_i , caused a net loss of 35–36% of the moisture initially present in the system.

Because (actual) air–water interfacial area and moisture content are inversely related within moisture ranges typical of natural systems, the substantial surfactant-induced drainage necessarily increases the interfacial area of the system over the course of the experiment, with larger surface tension changes creating proportionally more drainage and thus larger increases in interfacial area. Independent estimations of A_i – S_w relationships allow estimation of the increase in interfacial area produced by the surfactant-induced drainage. For example, high-resolution X-ray microtomography (μ CT) data for the same porous medium studied here¹⁵ suggest that the drainage induced in the 0.2 mM experiments, from ~ 83 to 41% S_w , would approximately triple the interfacial area relative to initial conditions, while even the lesser drainage induced in the 0.1 mM experiments would more than double the original interfacial area of the system. Similar analysis for the initially

dry experiment indicates that drainage would increase interfacial areas by $\sim 30\%$. These findings demonstrate that the assumptions of constant moisture content and interfacial area during miscible-displacement A_i measurement are substantially violated.

Effluent Flow Rate Perturbations. Perturbations to effluent flow rate relative to the initial steady-state conditions are shown in Figure 3a for representative wet experiments. For the highest surfactant concentration (0.2 mM), drainage resulted in a sharp surge in effluent flow rate immediately upon SDBS introduction to the column, followed by a return to steady-state flow after ~ 1 d as SDBS concentrations within the column became uniform and surface tension gradients diminished. At successively lower SDBS concentrations, the effluent surge was damped, its onset delayed, and its duration lengthened. The maximum effluent flow rates (averaged for replicate experiments) reached 15%, 27%, and 51% above steady-state conditions for the 0.05, 0.1, and 0.2 mM experiments, respectively. Over the time period relevant to t_{SDBS} determination (i.e., prior to SDBS $C/C_0 = 1$), and consequently of relevance to A_i determination, effluent flow rates were elevated by an average of 3%, 8%, and 12% for the 0.05, 0.1, and 0.2 mM SDBS wet experiments, respectively. The slower rate and lower magnitude of drainage observed for lower SDBS input concentrations is consistent with numerical modeling, indicating that smaller surface tension changes, and thus smaller capillary pressure gradients, cause smaller magnitude flow perturbations during one-dimensional miscible-displacement than do large surface tension changes.³⁴

Perturbations in effluent flow rate relative to the initial steady-state conditions for the dry system are shown in Figure 3b. Effluent flows during SDBS introduction to the initially dry system exhibited much greater fluctuations than for the wet system, even when smoothed over a longer time interval (8 h). We hypothesize that the greater fluctuations are due to the reduced hydraulic conductivity in the drier system, to the potential for air locks to develop, and to the lower signal-to-noise ratio for the smaller changes in column mass being monitored. The average effluent flow rate increase in the dry system was only 2% relative to steady-state conditions. Despite the modest flow rate increase, the cumulative drainage over the ~ 8 -day surfactant input removed more than 30% of the initial moisture from the system (Figure 1, inset) and, based on μ CT-derived A_i – S_w relationships described above, are expected to result in an $\sim 30\%$ increase in the interfacial area of the system.¹⁵ As was observed for the wet system, comparison of

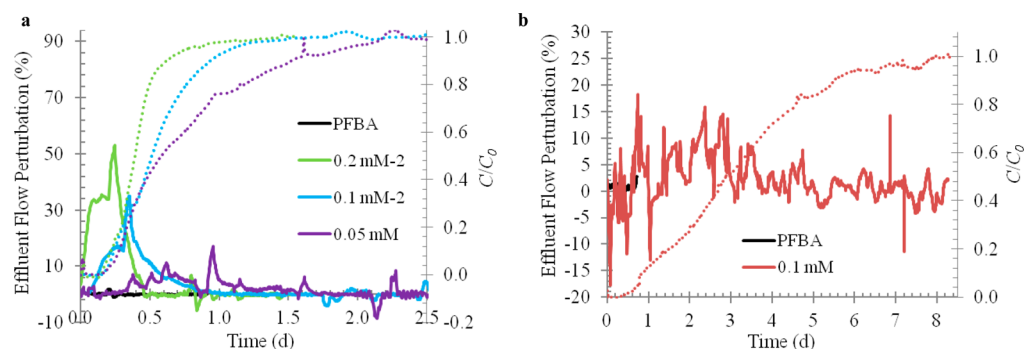


Figure 3. Perturbations in effluent flow rate (solid lines, left y-axes), expressed as % change compared to the steady-state condition, and SDBS arrival waves (dashed lines, right y-axes) for representative experiments for (a) wet and (b) dry (note the extended time axis) systems. Flow perturbation data (collected every 5 min) were smoothed using (a) 60-min or (b) 8-h boxcar averaging.

dry system effluent flow rate perturbations with SDBS arrival waves (Figure 3) shows that the bulk of the surfactant-induced drainage in the dry system was also completed before the effluent SDBS concentration reached $C/C_0 = 1$. Consequently, the surfactant-induced perturbations to bulk water flow, in addition to substantially altering actual interfacial areas, are likely to alter tracer arrival times and possibly influence R and A_i values.

Nonreactive Tracer Transport. The simultaneous-tracer experiment provides additional insight into the impact of surfactant-induced drainage on tracer transport. Figure 4 shows

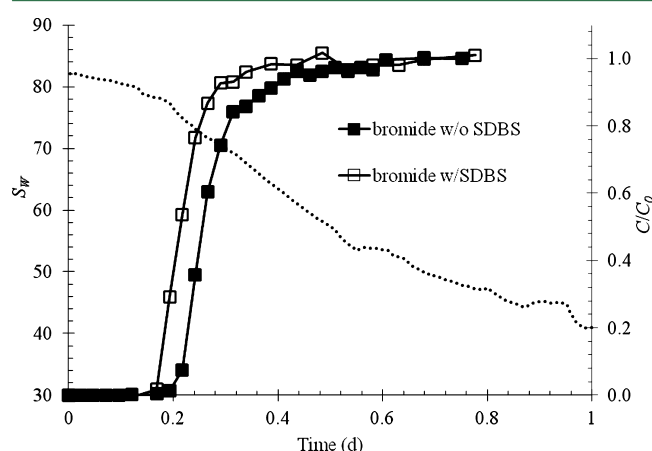


Figure 4. Column-average S_W versus time during simultaneous bromide/SDBS tracer introduction (dashed line, left y-axis) and bromide arrival waves (right y-axis) in the presence and absence of 0.1 mM SDBS.

bromide arrival waves in the presence and absence of SDBS, as well as the drainage observed during bromide breakthrough in the presence of SDBS. Bromide arrival time was decreased by 18% in the presence of 0.1 mM SDBS. The enhanced transport of bromide suggests that SDBS could also be hastened through the column as water drains, decreasing R and A_i . On the other hand, the larger air–water interface created by surfactant-induced drainage would serve to increase SDBS retardation, potentially increasing R and A_i . These competing effects will be discussed further with respect to calculated A_i . The bromide findings also have implications for the results of simultaneous-tracer vs sequential-tracer miscible-displacement A_i experiments, both of which have been reported. Because t_{SDBS} is normalized by $t_{\text{nonreactive}}$ in calculation of A_i (eqs 2 and 3), conducting miscible-displacement experiments in a sequential-tracer mode,^{8,17} in which only t_{SDBS} is influenced by surface tension changes, versus simultaneous-tracer mode,²⁰ in which both tracers would be influenced, alters the resulting R and A_i . Specifically, the observed reduction in $t_{\text{nonreactive}}$ during simultaneous-tracer input (0.1 mM SDBS) would increase the estimated A_i by an average of 61% relative to estimations from the equivalent sequential-tracer experiment.

Kim et al.²⁰ acknowledged the possibility that surfactant-induced flow might occur and could influence tracer transport. They suggested that in a simultaneous-tracer approach the nonreactive and interfacial tracers would experience the same surfactant-induced transient flow conditions, which would essentially compensate for the flow perturbations. Figure 4, however, reveals that during the bromide/SDBS pulse, drainage continued after bromide achieved $C/C_0 = 1$, such that even in

the simultaneous-tracer input case, the nonreactive and interfacial tracers experience different average flow conditions and moisture content. The magnitude of these differences between nonreactive and interfacial conditions will depend, in part, on the relative rate of transport of the nonreactive and interfacial tracers (i.e., on surfactant K_D and K_{IW}). Nevertheless, even if the enhanced transport of a nonreactive tracer in a simultaneous-tracer experiment were to mitigate the impact of surfactant-induced flow on the tracer arrival times, the problem of surfactant-induced drainage would still violate constant moisture content and interfacial area assumptions and complicate use of eq 3 for calculating A_i .

A_i Estimates. Arrival waves for wet sequential-tracer experiments (Figure 5) revealed that SDBS experienced greater

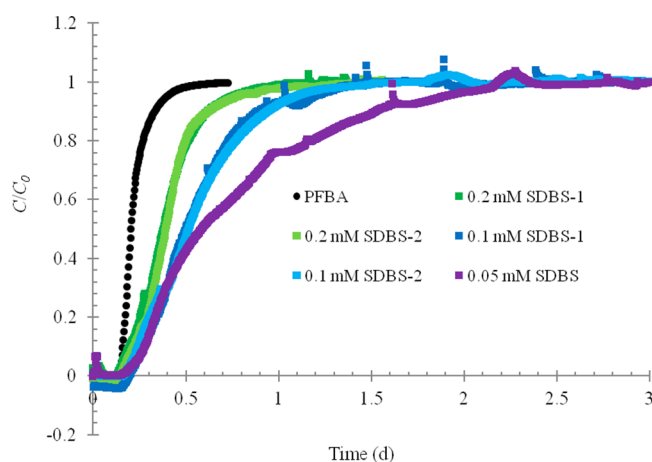


Figure 5. PFBA (representative) and SDBS arrival waves for sequential-tracer wet experiments. Arrival data for duplicate experiments overlap.

retardation at lower SDBS concentrations, consistent with the observed inverse concentration-dependence of both K_D and K_{IW} (see Supporting Information). Retardation factors ranged from 1.73 to 3.21, and despite some variation in initial moisture content, replicate experiments yielded acceptable precision (Figure 5 and Table 2). Conventionally, initial θ_w , which is assumed to be constant over the course of the experiment, is used in eq 3 to calculate A_i , which is similarly assumed to be constant during the experiment. Because our findings show that θ_w , and thereby (actual) interfacial areas, are substantially altered in the course of the measurement, it is not at all clear that A_i calculated in the conventional manner would provide a reasonable estimation of the air–water interfacial area of the initial (i.e., predrainage) system, as has been assumed, nor is it obvious that initial θ_w is the most appropriate value to describe the system in eq 3. Thus, we examined and compared A_i estimates based on the conventional initial θ_w , as well as time-averaged θ_w (i.e., prior to SDBS $C/C_0 = 1$).

A_i values calculated in the conventional manner (initial θ_w) for the wet system ranged from 63 to 101 cm^{-1} , differing by 60% across all SDBS input concentrations while only by ~20% between duplicate experiments. The larger variation in conventional A_i values across all experiments, as compared to the variation for duplicate experiments, provides some evidence that surfactant-induced drainage influences A_i . The estimates, however, did not exhibit a clear trend with respect to SDBS input concentration or magnitude of drainage (Table 2), which would be expected if the A_i estimates accurately reflected the

larger interfacial area conditions induced by drainage. The large variation in A_i and lack of a clear trend between A_i and the magnitude of drainage might be explained by the simultaneous occurrence of two surface-tension gradient influences on SDBS tracer transport: (1) by hastening SDBS transport through the column as water drains, SDBS arrival time is shortened; (2) by creating a larger air–water interface under the surfactant-drained conditions, interfacial retention is enhanced and SDBS arrival time is lengthened. Hypothetically acting in isolation, the first effect (induced drainage) would decrease R (and A_i), and the latter effect (increased interfacial area) would increase R (and A_i). Complicating matters is the concentration-dependence of surfactant K_D and K_{IW} , which would cause the relative proportion of surfactant molecules that are actively carried in the water phase and that are retained at air–water interfaces (subject to effects 1 and 2, respectively) to depend on surfactant concentration and to vary temporally and spatially during the experiment. Elucidating the relative contributions of these coupled, competing processes at various SDBS input concentrations would be useful in understanding the quantitative implications of surfactant-induced flow on A_i ; however, such an analysis, requiring development of new modeling approaches, is beyond the scope of the current work.

Because conventional surfactant miscible-displacement A_i values have served as a baseline for comparison in numerous experimental and modeling investigations of the air–water interface,^{7,11,15,16,19,21–29} evaluation of whether conventional A_i values tend to be over- or underestimates of actual values would be instructive. Unfortunately, a “consensus method” is not available for obtaining a “true” interfacial area value, due to a variety of methodological limitations.^{7,11,18,19} Similarity with true values aside, direct quantitative comparison of the various A_i methods, as attempted by Costanza-Robinson and Brusseau,¹¹ has proven difficult because multiple methods have rarely been applied to a porous media system in common. A few studies, however, allow comparison of conventional surfactant-miscible displacement A_i with values obtained via μ CT imaging. For example, the conventional miscible-displacement A_i estimates reported here are 2.5–4 times larger than μ CT A_i estimates for the same porous medium and similar (initial) moisture conditions.¹⁵ This finding is consistent with the discrepancy between surfactant miscible-displacement- and μ CT- A_i estimates reported by Brusseau et al.¹⁷ In contrast, conventional surfactant miscible-displacement A_i values reported by Kim et al.²⁰ were lower than A_i values predicted for the same porous medium using a μ CT-based empirical model that incorporated porous medium-specific properties (e.g., surface areas).¹⁵ The cases in which surfactant miscible-displacement A_i values exceed μ CT estimates^{15,17} used sequential-tracer input, while Kim et al.,²⁰ reporting smaller miscible-displacement A_i as compared to μ CT, relied upon simultaneous-tracer input. This is the opposite of what might be expected, because sequential-tracer experiments would be expected to yield lower A_i due to the longer $t_{\text{nonreactive}}$ measured in the absence of surfactant-induced drainage. Thus, while the most direct comparison available (μ CT estimates of A_i for the same medium studied here) suggest that conventional miscible-displacement estimates reported here are approximately two times too high, the available data are insufficient for drawing a general conclusion regarding the magnitude of error in conventional A_i estimates.

Because time-averaged θ_w values more accurately represent the moisture content of the experimental system during the

course of measurement, we briefly examined the impact of using this θ_w value in eq 3. Time-averaged A_i estimates were lower than conventional A_i , ranging from 29 to 63 cm^{−1} (Table 2) and correspond more closely to the magnitude of μ CT-based A_i estimates. The A_i data do not exhibit a definitive relationship with time-average moisture content, however, and if anything, are correlated positively rather than inversely. We conclude that use of time-averaged θ_w for A_i estimation does not improve the reliability of A_i values.

As has been suggested previously, surfactant miscible-displacement experiments would be improved by reducing surfactant concentrations or eliminating surface tension changes altogether by using a radiolabeled surfactant as the interfacial tracer and displacing pore water that already contains the same concentration of unradiolabeled surfactant.^{7,20} However, the critical need for such improvements has been underestimated and the complications of surfactant-induced flow largely ignored. Further work is needed to examine the feasibility of such proposed improvements for an already time-intensive and complicated technique.

In this work, we have demonstrated that the effects of surface tension changes associated with surfactant miscible-displacement experiments are considerably larger than previously recognized and cause several fundamental method assumptions to be violated, including assumptions of steady-state flow, of constant moisture content and interfacial area, and of the equivalence of transport conditions for nonreactive and interfacial tracers. An important distinction, due to surfactant-induced flow, between conducting experiments in sequential- vs simultaneous-tracer modes was also established. Although further work is required to quantify the net impact of these complex processes on A_i , our findings cast considerable doubt on the reliability of surfactant miscible-displacement A_i values. Accordingly, the use of surfactant miscible-displacement A_i values to benchmark other techniques or mathematical models that seek to simulate interfacial features and processes should be done with caution, while conclusions that have relied on such comparisons should be revisited. Further assessment of the relative reliability of alternative A_i measurement methods, as well as the development of innovative A_i measurement techniques, including improvements to surfactant miscible-displacement methods, is crucial to improved understanding of interfacial processes in porous media.

■ ASSOCIATED CONTENT

● Supporting Information

Text and two figures describing miscible-displacement boundary conditions and determination of K_D and K_{IW} . This material is available free of charge via the Internet at <http://pubs.acs.org>.

■ AUTHOR INFORMATION

Corresponding Author

*Phone: 802/443-5571; fax: 802/443-2072; e-mail: mcostanz@middlebury.edu.

Notes

The authors declare no competing financial interest.

■ ACKNOWLEDGMENTS

The authors gratefully acknowledge the Environmental Microbiology Group at The University of Arizona for surface tension analysis. We thank two anonymous reviewers for their constructive critique and thoughtful suggestions. This research

was supported by grants provided by the National Science Foundation (EAR-0711499), the Petroleum Research Fund (47012-GB8), the University of North Carolina Wilmington (Summer Research Initiative), and Middlebury College.

REFERENCES

- (1) Kim, H.; Annable, M. D.; Rao, P. S. C. Influence of air–water interfacial adsorption and gas-phase partitioning on the transport of organic chemicals in unsaturated porous media. *Environ. Sci. Technol.* **1998**, *32* (9), 1253–1259.
- (2) Kim, H.; Annable, M. D.; Rao, P. S. C. Gaseous transport of volatile organic chemicals in unsaturated porous media: Effect of water-partitioning and air–water interfacial adsorption. *Environ. Sci. Technol.* **2001**, *35* (22), 4457–4462.
- (3) Brusseau, M. L.; Popovicova, J.; Silva, J. A. K. Characterizing gas–water interfacial and bulk-water partitioning for gas-phase transport of organic contaminants in unsaturated porous media. *Environ. Sci. Technol.* **1997**, *31*, 1645–1649.
- (4) Anwar, A. H. M. F.; Bettahar, M.; Matsubayashi, U. A method for determining air–water interfacial area in variably saturated porous media. *J. Contam. Hydrol.* **2000**, *43* (2), 129–146.
- (5) Karkare, M. V.; Fort, T. Determination of the air–water interfacial area in wet “unsaturated” porous media. *Langmuir* **1996**, *12* (8), 2041–2044.
- (6) Schaefer, C. E.; DiCarlo, D. A.; Blunt, M. J. Experimental measurement of air–water interfacial area during gravity drainage and secondary imbibition in porous media. *Water Resour. Res.* **2000**, *36* (4), 885–890.
- (7) Chen, L.; Kibbey, T. C. G. Measurement of air–water interfacial area for multiple hysteretic drainage curves in an unsaturated fine sand. *Langmuir* **2006**, *22* (16), 6874–6880.
- (8) Saripalli, K. P.; Kim, H.; Rao, P. S. C.; Annable, M. D. Measurement of specific fluid–fluid interfacial areas of immiscible fluids in porous media. *Environ. Sci. Technol.* **1997**, *31* (3), 932–936.
- (9) Kim, H.; Rao, P. S. C.; Annable, M. D. Gaseous tracer technique for estimating air–water interfacial areas and interface mobility. *Soil Sci. Soc. Am. J.* **1999**, *63* (6), 1554–1560.
- (10) Okamura, J. P.; Sawyer, D. T. Gas chromatographic studies of sorptive interactions of normal and halogenated hydrocarbons with water-modified soil, silica, and Chromosorb W. *Anal. Chem.* **1973**, *45*, 80–84.
- (11) Costanza-Robinson, M. S.; Brusseau, M. L. Air–water interfacial areas in unsaturated soils: Evaluation of interfacial domains. *Water Resour. Res.* **2002**, *38* (10), 1195–1211.
- (12) Sung, M.; Chen, B.-H. Using aliphatic alcohols as gaseous tracers in determination of water contents and air–water interfacial areas in unsaturated sands. *J. Contam. Hydrol.* **2011**, *126* (3–4), 226–234.
- (13) Cheng, J.-T.; Pyrak-Nolte, L. J.; Nolte, D. D.; Giordano, N. J. Linking pressure and saturation through interfacial areas in porous media. *Geophys. Res. Lett.* **2004**, *31*, L08502.
- (14) Brusseau, M. L.; Peng, S.; Schnaar, G.; Costanza-Robinson, M. S. Relationships among air–water interfacial area, capillary pressure, and water saturation for a sandy porous medium. *Water Resour. Res.* **2006**, *42* (3), W03501.
- (15) Costanza-Robinson, M. S.; Harrold, K. H.; Lieb-Lappen, R. M. X-ray microtomography determination of air–water interfacial area–water saturation relationships in sandy porous media. *Environ. Sci. Technol.* **2008**, *42*, 2949–2956.
- (16) Culligan, K. A.; Wildenschild, D.; Christensen, B. S. B.; Gray, W. G.; Rivers, M. L.; Tompson, A. F. B. Interfacial area measurements for unsaturated flow through a porous medium. *Water Resour. Res.* **2004**, *40* (12), W12413.
- (17) Brusseau, M. L.; Peng, S.; Schnaar, G.; Murao, A. Measuring air–water interfacial areas with X-ray microtomography and interfacial partitioning tracer tests. *Environ. Sci. Technol.* **2007**, *41* (6), 1956–1961.
- (18) Brusseau, M. L.; Narter, M.; Janousek, H. Interfacial partitioning tracer test measurements of organic-liquid/water interfacial areas: Application to soils and the influence of surface roughness. *Environ. Sci. Technol.* **2010**, *44* (19), 7596–7600.
- (19) Bryant, S.; Johnson, A. Bulk and film contributions to fluid/fluid interfacial area in granular media. *Chem. Eng. Commun.* **2004**, *191* (12), 1660–1670.
- (20) Kim, H.; Rao, P. S. C.; Annable, M. D. Determination of effective air–water interfacial area in partially saturated porous media using surfactant adsorption. *Water Resour. Res.* **1997**, *33* (12), 2705–2711.
- (21) Chen, D.; Pyrak-Nolte, L. J.; Griffin, J.; Giordano, N. J. Measurement of interfacial area per volume for drainage and imbibition. *Water Resour. Res.* **2007**, *43* (12), W12504.
- (22) Peng, S.; Brusseau, M. L. Impact of soil texture on air–water interfacial areas in unsaturated sandy porous media. *Water Resour. Res.* **2005**, *41* (3), W03021.
- (23) Costanza, M. S.; Brusseau, M. L. Contaminant vapor adsorption at the gas–water interface in soils. *Environ. Sci. Technol.* **2000**, *34* (1), 1–11.
- (24) Oostrom, M.; White, M. D.; Brusseau, M. L. Theoretical estimation of free and entrapped nonwetting-wetting fluid interfacial areas in porous media. *Adv. Water Resour.* **2001**, *24*, 887–898.
- (25) Dalla, E.; Hilpert, M.; Miller, C. T. Computation of the interfacial area for two-fluid porous medium systems. *J. Contam. Hydrol.* **2002**, *56*, 25–48.
- (26) Tuller, M.; Or, D.; Dudley, L. M. Adsorption and capillary condensation in porous media: Liquid retention and interfacial configurations in angular pores. *Water Resour. Res.* **1999**, *35*, 1949–1964.
- (27) Or, D.; Tuller, M. Liquid retention and interfacial area in variably saturated porous media: Upscaling from single-pore to sample-scale model. *Water Resour. Res.* **1999**, *35* (12), 3591–3605.
- (28) Berkowitz, B.; Hansen, D. P. A numerical study of the distribution of water in partially saturated porous rock. *Transp. Porous Media* **2001**, *45*, 303–319.
- (29) Porter, M. L.; Wildenschild, D.; Grant, G.; Gerhard, J. I. Measurement and prediction of the relationship between capillary pressure, saturation, and interfacial area in a NAPL–water–glass bead system. *Water Resour. Res.* **2010**, *46*, 10.
- (30) Desai, F. N.; Demond, A. H.; Hayes, K. F. Influence of surfactant sorption on capillary pressure–saturation relationships. In *Transport and remediation of subsurface contaminants*; Sabatini, D. A.; Knox, R. C., Eds.; American Chemical Society: Washington, DC, 1992; Vol. 491.
- (31) Henry, E. J.; Smith, J. E. Surfactant-induced flow phenomena in the vadose zone: A review of data and numerical modeling. *Vadose Zone J.* **2003**, *2* (2), 154–167.
- (32) Bashir, R.; Smith, J. E.; Stolle, D. F. Surfactant-induced unsaturated flow: Instrumented horizontal flow experiment and hysteretic modeling. *Soil Sci. Soc. Am. J.* **2008**, *72* (6), 1510–1519.
- (33) Costanza-Robinson, M. S.; Estabrook, B. D.; Fouhey, D. F. Representative elementary volume estimation for porosity, moisture saturation, and air–water interfacial areas in unsaturated porous media: Data quality implications. *Water Resour. Res.* **2011**, *47*, W07513.
- (34) Smith, J. E.; Gillham, R. W. The effect of concentration-dependent surface tension on the flow of water and transport of dissolved organic compounds: A pressure head-based formulation and numerical model. *Water Resour. Res.* **1994**, *30* (2), 343–354.